Decentralized Energy Management Concept for Urban Charging Hubs with Multiple V2G Aggregators

Erdem Gümrükcü, *Student Member, IEEE,* Jonatan Ralf Axel Klemets, Jon Are Suul, *Member, IEEE,* Ferdinanda Ponci, *Senior Member, IEEE,* Antonello Monti, *Senior Member, IEEE*

***Abstract*—This work introduces a decentralized management concept for the urban charging hubs (UCHs) where electric vehicles (EVs) can access multiple charger clusters, each controlled by an aggregator. The given day ahead schedules (DASs) and peak power limits (PPLs) of the aggregators providing grid-to-vehicle (G2V) and vehicle-to-grid (V2G) services can constrain the energy supply. A suitable energy management concept is required to prevent the impact of supply limitations on EV users. In the proposed approach, an electromobility operator (EMO) acting as an authorized entity, allocates incoming EVs into the charger clusters in the UCH. The EMO executes a smart routing (SR) algorithm that jointly optimizes the cluster allocations and charging schedules, minimizing the charging cost for the given dynamic price signals produced by the aggregators. For real-time charging control (RTC) of the charging units, each aggregator solves an optimization problem with periodically updated parameters given by the DAS/PPLs and charging commitments. This work demonstrates the effectiveness of the proposed concept through comparisons against benchmark strategies without SR and RTC. The results highlight that the proposed concept reduces the deviations from the DASs and the violations of PPLs while significantly decreasing unfulfilled charging demand and unscheduled discharge from EV batteries.**

GLOSSARY

Frequently used abbreviations

DAS	Day ahead schedule
DP	Dynamic price
EMO	Electromobility operator
EV	Electric vehicle
RTC	Real time (charging) control
SOC	State-of-charge
SR	Smart routing
UCH	Urban charging hub
V2G	Vehicle-to-grid

Manuscript received May 23, 2022; revised August 17, 2022; accepted September 14, 2022. Date of publication MM DD, YY; date of current version MM DD YY. This work was supported by the project ALigN, funded by the Federal Ministry for Economic Affairs and Energy of Germany (Grant Number: 01MZ18006G) and the project FuChar (295133/E20) funded by Norweigan Research Council. *(Corresponding author: Erdem Gümrükcü)*

E. Gümrükcü , F. Ponci and A. Monti are with the Intitute for Automation of Complex Power Systems, E.ON Energy Research Center, RWTH Aachen University, Aachen, Germany (email: [erdem.guemruekcue, fponci, amonti]@eonerc.rwth-aachen.de)

Jonatan Klemets is with SINTEF Energy Research, Trondheim, Norway. (email: jonatan.klemets@sintef.no)

Jon Are Suul is with SINTEF Energy Research, Trondheim, Norway, and also with the Department of Engineering Cybernetics, Norwegian University of Science and Technology, Trondheim, Norway.(email: jon.a.suul@sintef.no)

Indices

c	Cluster controlled by an aggregator
u	Charging unit
v	Electric vehicle

Dynamic Pricing

κ_c	The regular time-of-use tariff of c
$\underline{\pi_c}$,$\overline{\pi_c}$	Peak power limits of c
$\underline{L_c}$,$\overline{L_c}$	Lower and upper limits of desired consumption range of c
φ_c	Day ahead schedule of c

Smart Routing

$\omega_{c,v}$	DP signal calculated by c for v
$\overline{E_v^-}$	V2G allowance of v
$\underline{S_v}$,$\overline{S_v}$	Lower and upper limit of desired SOC range v
A_v, D_v	Arrival and departure time of v
E_v	Battery capacity of v
P_c^-,P_c^+	Maximum discharge and charge rating of the charger type of cluster c
p_v	Charging schedule of v
$S_v(A_v)$	Arrival SOC of v
$S_v(D_v)$	Target SOC of v
$x_{v,c}$	Binary variable representing allocation of v to c
x_v^+	Binary variable representing positive power (charging) to v

Real Time Charging Control

η_u^-,η_u^+	Discharging and charging efficiency of u
$\underline{P_c}$,$\overline{P_c}$	Lower and upper limits of the aggregate net consumption of c
p_u	Net power to the EV connected in u
P_u^-,P_u^+	Maximum power that can be discharged from and charged to the EV battery by u
p_u^-,p_u^+	Negative (discharging) and positive (charging) power to the EV connected in u
S_u^*	Reference SOC of the EV in u
s_u	SOC of the EV in u
x_u^+	Binary variable representing positive power (charging) to the EV in u

I. INTRODUCTION

Electric vehicles (EVs) are becoming more and more popular in many countries.For instance, in Germany, plug-in EVs (plug-in hybrid plus full-electric vehicles) made up only 2% of the new car registrations in 2018. Since then, the share

of plug-in EVs have been growing continuously and reached 26% in 2021 [1]. Furthermore, the share of full-electric cars reached 64.5% of all new cars sold in Norway in 2021 [2].The increasing penetration of EVs also imposes the need for expansion of charging infrastructure.

It is safe to foresee that most urban parking lots (PLs) will accommodate EV charging infrastructure in the future. An urban PL having a number of EV chargers is a natural aggregation environment for EVs. Therefore, densely populated urban areas having multiple public PLs in short perimeters are likely to develop into urban charging hubs (UCHs) with multiple aggregation units. These aggregation units will be referred to as charger clusters in the following. Especially when the charger clusters in the UCH share a distribution grid under the same secondary substation, uncontrolled charging can lead to serious grid problems, such as overloading on substation transformers, thermal stress on the lines, voltage drops, voltage unbalance, power losses and rising peak demand [3]. Suitable operational strategies will be required to achieve coordination between the charger clusters in the future UCHs.

A. *Statement of problem*

This work addresses the energy management problem of future UCHs with multiple aggregators. In general, aggregators provide a single interface point for utilities to interact with a group of distributed energy resources across the network and thus facilitate cooperative control of large-scale systems [4]. In a UCH, each PL operator responsible for a cluster of charging units can act as an aggregator. In addition to providing G2V charging to the EVs, these aggregators can offer V2G services to the energy market such as frequency control reserve [5].

An UCH with multiple aggregators presents a unique energy flexibility management problem. On the one hand, such a system would be a competitive market as each aggregator aims to maximize its energy sales to EVs. On the other hand, uncoordinated operation of selfish aggregators may lead to lose-lose situations. The lack of coordination may result in serious problems in the power distribution grid shared by the charger clusters. For the cooperative operation of UCHs with competitive aggregators, it is necessary to identify relevant control capabilities and develop suitable algorithms.

B. *Literature review*

There exists a considerable body of literature on coordinated EV charging, emphasizing that it enables peak flattening, cost reduction, and charging with renewable energy in various use cases [6]–[8]. The most relevant references for the scenario addressed in this work are in the following areas: multi-aggregator systems, networked microgrids, and large PLs. This section mentions a few representative examples to highlight the need for an original approach for the UCHs.

The authors of [9] propose a hierarchical multi-agent framework where the grid operator of a specific region (i.e., higher-level agent) solves a designated optimal power flow problem to assign peak power constraints to the aggregators (i.e., lower-level agents). The aggregators organize their EV charging activities considering these constraints. Kaur et al. present a similar hierarchical approach to provide V2G-based frequency support in scenarios with multiple EV aggregators in [10]. Similar hierarchical approaches are also applied in incentive-based frameworks. For instance, Yi et al. formulate the intelligent behavior of the virtual power plants (VPP) agents and the aggregators as two layers of a hierarchical system [11]. In the higher layer, the VPP agent acts as a price-maker; in the lower layer, the aggregators optimize the schedules of the controllable devices according to the price curves issued by the VPP agent. Li et al. consider a similar approach for the scenario with a load-serving entity that purchases electricity from the wholesale market and sells it to multiple aggregators [12]. In the strategy proposed in [12], the aggregators are rewarded with customer coupons when they contribute to the peak shaving objective of the load-serving entity. Kok et al. apply locational marginal pricing to coordinate the operation of multiple aggregators in a distribution network [13].

Both control- and incentive-based methods developed in previous studies provide valuable perspectives on flexibility management in multi-aggregator systems. That said, the problem described in Section I-A has a peculiar flexibility dimension that does not exist in most multi-aggregator systems. Typically, a UCH would have multiple available charger clusters within proximity of the intended destination of the EV driver. Therefore, the incoming EVs can be allocated (i.e., routed) within the UCH to support the aggregator goals. It is important to note that this is not the same problem as the charging station selection in inter-city trips (e.g., [14], [15]). In such trips, the temporal flexibility is limited since EV drivers usually prefer fast charging to reduce waiting time. In the UCH, fast charging is not always a requirement because EV drivers can spend time longer than the minimum required for recharging EV batteries. Hence, the routing problem in UCHs will be associated with a scheduling problem.

One can draw an analogy between UCHs with multiple charger clusters and networked microgrids. A networked microgrid is a community of microgrids collaborating for providing reliable and low-cost power supply to the end customers and offering services in ancillary markets [16]. When such a community consists of closely located microgrids, it would be beneficial to manage the distribution of incoming EVs to support the community's objectives. Previous studies on networked microgrids (e.g. [17], [18]) have almost exclusively focused on the temporal flexibility of EV charging. Only a few works in the literature demonstrate the benefits of active mobility management in networked microgrids. The authors of [19] consider EVs as a solution to increase the resilience of microgrids and design a scheme where EVs travel between microgrids to supply power to the sections that lost connection from the main grid during a contingency. The strategy proposed in [19] requires connected EVs to leave their spots and travel to other microgrids multiple times; however, it does not include active routing management of incoming EVs. Another recent publication introduces a charging station recommendation algorithm minimizing the load factor unbalance between individual microgrids [20]. However, the algorithm proposed in [20] does not optimize the charging schedules of EVs. Therefore, it neglects a crucial dimension of flexibility

in the management problem.

A series of recent studies indicated the importance of active mobility management in large PLs with clustered EV charging systems. In [21], the authors address a generic topology with multiple charger clusters fed by dedicated feeders under peak power constraints. The referred work introduces a centralized management strategy based on cascaded optimization of incoming EVs' schedules and allocation into clusters. The same parking operator owns all the charger clusters in the scenario investigated in [21]. Therefore, the allocation step minimizes the inter-cluster unbalances to avoid peak power violation. The authors implement the same approach also in [22] for charging stations with grid side interface based on modular multilevel converters (MMC). This approach reduces the unbalances between the MMC arms where charging units arc clustered. Nevertheless, since the strategy proposed in [21], [22] does not exploit V2G transfer, it is not a generally applicable solution for the UCHs with aggregators providing grid services. Furthermore, balancing between clusters, as pursued in [21] and [22], is not necessarily desired in an environment with multiple competitive aggregators. When an aggregator offers cheaper charging, the allocation of the incoming EV to this aggregator's cluster would be more reasonable.

To summarize, an UCH with multiple aggregators have similarities with other multi-aggregator systems and networked microgrids. It is beneficial to consider EV mobility a controllable feature jointly with temporal flexibility to support the cooperative objectives of the aggregators operating charger clusters. The existing routing management frameworks in the literature do not meet the requirements of a scenario where aggregators compete for EVs during daily operation while providing V2G services. All things considered, the future UCHs with multiple aggregators present a unique management problem. To best of the authors' knowledge, no prior studies have examined this problem.

C. Statement of Contributions

In the light of the presented literature review, the overall goal of this work is to develop an overarching framework to manage UCHs with multiple aggregators. The concept developed toward this goal is summarized in Fig. 1 by illustrating the interactions between the involved parties. In this concept, each aggregator is responsible for charging coordination of a particular cluster and the electromobility operator (EMO) is responsible for allocating incoming EVs to clusters in the UCH. The intelligent behavior of EMO and aggregators are represented by smart routing (SR) and real-time control (RTC) algorithms respectively.

The SR algorithm is executed upon reservation requests of EV drivers that will visit the UCH. At this step, the aggregators send their individualized dynamic price (DP) signals to the EMO. Through DP signals, each aggregator indicates the desired consumption profiles in its cluster by assigning high prices for the periods when the additional charging load must be avoided due to given day ahead schedules (DASs) or peak power limits (PPLs). The SR strategy jointly optimizes the allocation of incoming EVs into charger clusters and their charging schedules. This approach prioritizes the EV users' interests and therefore, aims at charging cost minimization under the given DP signals. Aggregators control the real-time set points of the charging units in their clusters by executing RTC algorithm periodically. RTC expedites or suspends charging of certain EVs if the given DAS or PPL requires deviation from the individual-optimal charging schedules of the EVs, which are calculated at the SR step.

The main technical contributions of this work are as follows: 1) It introduces a management concept for UCHs with multiple cluster, which defines specific roles for the aggregators and EMO in a competitive market. 2) It formalizes the intelligent behavior of the interacting parties through dynamic pricing, SR and RTC algorithms. 3) It defines performance metrics to quantify the degree at which the cooperative objectives of the aggregators are met. 4) It assesses the proposed strategy in test scenarios under capacity constraints, limiting energy supply potential of UCHs, and compares the strategy against relevant benchmarks.

II. Individualized Dynamic Pricing

A. Context

Individualized dynamic pricing is a component of the developed energy management concept. It helps the aggregators to achieve their desired consumption profiles and the EMO to optimize the allocation of incoming EVs into the charger clusters. Each aggregator in the UCH determines its own DP signal. A DP signal includes time-dependent cost coefficients for EV charging in a cluster controlled by a particular aggregator. Aggregators update their DP signals based on the new conditions, such as new charging commitments or renewable forecast. This approach is in line with the usual tendency in the literature (e.g., [8], [17], [23]), where DP signals are deemed as indicators of the desired consumption profiles.

In the considered scenarios, the aggregators purchase electricity in the day ahead market as suggested by many literature works (e.g. [24]). Day ahead schedules (DASs) and peak power limits (PPLs) define the desired consumption profiles of the aggregators during intra-day operation. The processes underlying the DAS and PPL specifications are not within the scope of this work. This work assumes that DASs and PPLs are given scenario inputs and there exist incentives for aggregators to accept them. When producing DP signals, the aggregators assign high values for the periods where they should avoid additional power consumption due to the given DASs or PPLs.

In the developed concept, when the EMO of UCH receives a reservation request from an EV, it calls aggregators in the system for DP signals. With the provided DP signals, it solves an optimization problem and routes the incoming EV into the cluster offering the minimum charging price for the requested amount of charging demand. This step jointly optimizes charging schedules and cluster (i.e., aggregator) allocations. Section III-A explains the relationship between the individualized dynamic pricing and SR in greater detail.

Besides indicating the desired consumption profiles and enabling SR, DP signals could provide a quantitative basis for billing charging services. The billing strategy can be an

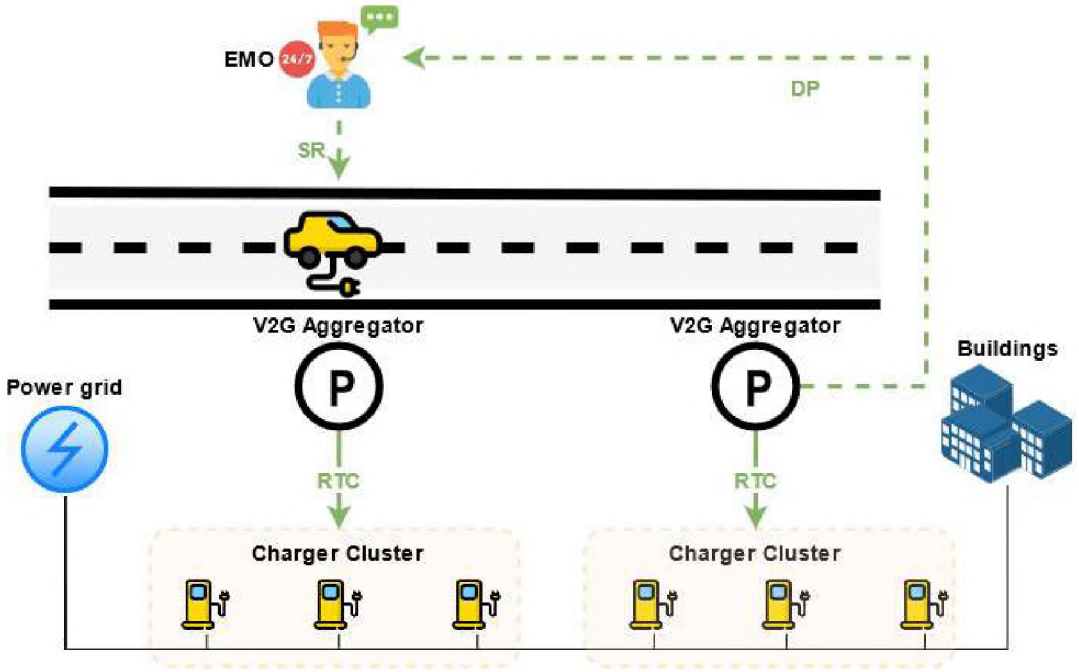

Fig. 1. Distributed management concept for UCHs. Dashed and solid arrows represent occasionally and periodically executed algorithms respectively.

essential element of the competition between the aggregators as the charging price is an incentive factor that affects the EV drivers' selection among alternative suppliers. However, this work focuses on the energy management of UCHs; the billing and competition strategies of the aggregators are not within the scope. Therefore, individual dynamic pricing is only a component of the management concept.

B. Generic Formulation for Individualized Dynamic Pricing

Whenever the EMO informs the aggregators about a reservation request, each aggregator having an available charger in its cluster generates a DP signal. In the following, $\omega_{c,v}$ represents the DP signal generated by the aggregator controlling the cluster c for the EV v. In fact, $\omega_{c,v}$ is a time-dependent parameter, with $\omega_{c,v}(t)$ representing the price for kWh EV charging at a time interval represented by t. The following piece-wise function formalizes the rules to determine DP signals, $\omega_{c,v}(t)$:

$$= \begin{cases} \kappa_c(t) & \underline{L_c}(t) < \hat{p_{c,v}}(t) < \overline{L_c}(t) \\ \underline{\kappa_c}(t) - F^- \cdot (\underline{L_c}(t) - \hat{p_{c,v}}(t)) & \hat{p_{c,v}}(t) \leq \underline{L_c}(t) \\ \overline{\kappa_c}(t) + F^+ \cdot (\hat{p_{c,v}}(t) - \underline{L_c}(t)) & \hat{p_{c,v}}(t) \geq \overline{L_c}(t) \end{cases} \quad (1)$$

where the parameters $\overline{L_c}(t)$ and $\underline{L_c}(t)$ represent the upper and lower limits of the desired power consumption of the c. The sections II-C and II-D explain how the aggregator controlling c determines $\overline{L_c}(t)$ and $\underline{L_c}(t)$ under given DAS and PPL. $\hat{p_{c,v}}(t)$ is the scheduled aggregate consumption of c for t. v index in this parameter denotes that it is an individualized parameter for the EV represented by v; hence it changes with the new charging commitments. $\hat{p_{c,v}}(t)$ has positive values if c will withdraw power from the public grid at t (power flow from grid to cluster) and negative values if it will inject power to the grid (power flow from cluster to grid).

The piece-wise function (1) indicates that three cases are distinguished in calculation of $\omega_{c,v}(t)$. The first case occurs when the scheduled net consumption of the cluster is within the desired range specified by $\underline{L_c}(t)$ and $\overline{L_c}(t)$. For the t steps where this condition is met, $\omega_{c,v}(t)$ is equal to the regular time-of-use tariff of the aggregator, $\kappa_c(t)$. The second and third cases indicate that $\hat{p_{c,v}}(t)$ is, respectively, less than $\underline{L_c}(t)$ and larger than $\overline{L_c}(t)$. In these cases, $\kappa_c(t)$ are overridden by, respectively, smaller and larger cost coefficients.

To ensure that the charging is more attractive when the lower limit is missed (deficit consumption), the cost coefficient for all t with deficit consumption must be smaller than the minimum of the electricity purchase tariff of the aggregator, $\underline{\kappa_c}(t)$. In the proposed approach, these adjustments are done by considering the amount of deficit $(\underline{L_c}(t) - \hat{p_{c,v}}(t))$ and reducing the coefficients proportionally to the deficit consumption. In the mathematical formulation F^- is the discount factor for compensating each kW of deficit consumption. With the same principle, the coefficients for t with excessive consumption must be larger than the maximum of the tariff of the aggregator, $\underline{\kappa_c}(t)$, and the coefficients must be increased proportionally to the excessive consumption, that is $(\underline{L_c}(t) - \hat{p_{c,v}}(t))$. In (1), F^+ represents the markup factor for compensating each kW of excessive consumption.

The following subsections elaborate the implementation of the generic DP formulation in two use cases where DASs and PPLs of the aggregators determine $\underline{L_c}$ and $\overline{L_c}$.

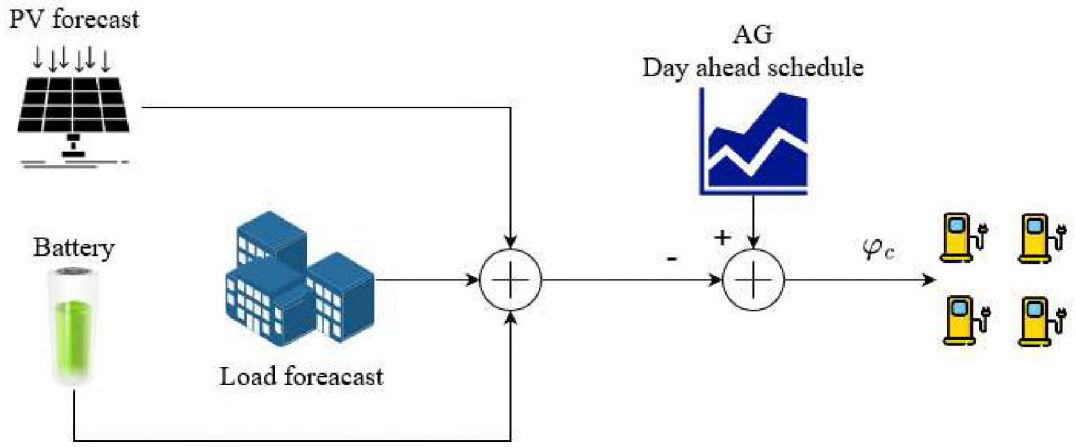

Fig. 2. DASs of aggregators and their relation to charger clusters

C. DP calculation under day ahead schedules

The literature pertaining to the aggregators often emphasizes day-ahead scheduling as an enabler for energy producers' participation in the energy flexibility market [25]. For this reason, we considered the scenarios where each aggregator in a UCH has a given DAS. In this case, the DAS defines the reference loading profile of the charger cluster operated by the aggregator. It is important to note that the policies generating the aggregators' DASs are not within the scope of this work. Likewise, the control of other flexible assets such as stationary batteries is assumed to be an independent process. Therefore, the DASs are linked to the DP as exogenous inputs. With c indicating a particular cluster, the reference schedule for this cluster, φ_c, is the residual power after subtracting the net consumption of all other electrical entities in the control of the aggregator from the DAS as shown in Figure 2.

When an aggregator has a given DAS, φ_c is considered to be as both the upper $\overline{L_c}$ and lower limits $\underline{L_c}$ of desired net consumption of the cluster c as shown in (2). In this case, the aggregator would tend to lower charging prices for t where the scheduled consumption of the cluster indicates a power consumption less than the given DAS (i.e., $\hat{p_{c,v}}(t) < \varphi_c$) and vice versa.

$$\overline{L_c}(t) = \underline{L_c}(t) = \varphi_c \tag{2}$$

D. DP calculation under peak power limits

Peak shaving is a common practice in power systems. It is particularly beneficial for the grid operators as it helps avoiding grid congestion and improving operational efficiency. It also offers some direct incentives to the energy consumers (e.g., reduced capacity fees) and indirect benefits (e.g., grid reliability). In the considered use case, the aggregators are assumed to have agreements with other entities such as energy providers or grid operators, and thus, they are obliged to keep their net power consumption between the specified limits. However, the procedure for the specification of the PPLs is not within the scope of this work. Therefore, the PPLs are scenario parameters. π_c^+ is the upper limit of the power that cluster c is allowed to withdraw from the grid at t, and π_c^- the upper limit power that c can inject at t. Therefore these parameters define $\overline{L_c}$ and $\underline{L_c}$ as follows:

$$\overline{L_c}(t) = \pi_c^+ \tag{3}$$

$$\underline{L_c}(t) = -\pi_c^- \tag{4}$$

III. Smart Routing

The management concept considered in this work entitles the UCH's electromobility operator (EMO) to allocate the incoming EVs to charger clusters, each operated by an aggregator. In the smart routing (SR) strategy, the EMO prioritizes the economic interests of EV drivers. Based on the DP signals provided by the aggregators, it finds the optimal combination of cluster selection and charging profile (reference schedule), minimizing the charging cost for the incoming EV. Since DP signals indicate when and where additional charging load should be motivated/avoided, SR helps track DASs and keep the charger clusters' consumption under PPLs.

This work applies the proposed SR strategy only in scenarios where each aggregator operates a cluster of charging units (CUs) with identical power ratings. Nevertheless, this strategy can also be applied in scenarios where the aggregators have CUs with different power ratings in their portolio. In such a scenario, a single aggregator can calculate multiple DP signals distinguishing the power ratings of the available CUs. It would be reasonable for the aggregators to assign the larger prices to the CUs with the higher power rating. However, such quantification is not within the scope of this work.

A. System architecture

For the implementation of the developed SR strategy, the system architecture illustrated in Figure 3 is envisioned. This architecture focuses on the functional relationships between the interacting entities, and thus it describes the input/outputs exchanged by the EV drivers, EMO, and aggregators. A system design with a detailed description of necessary software/hardware components and communication standards is

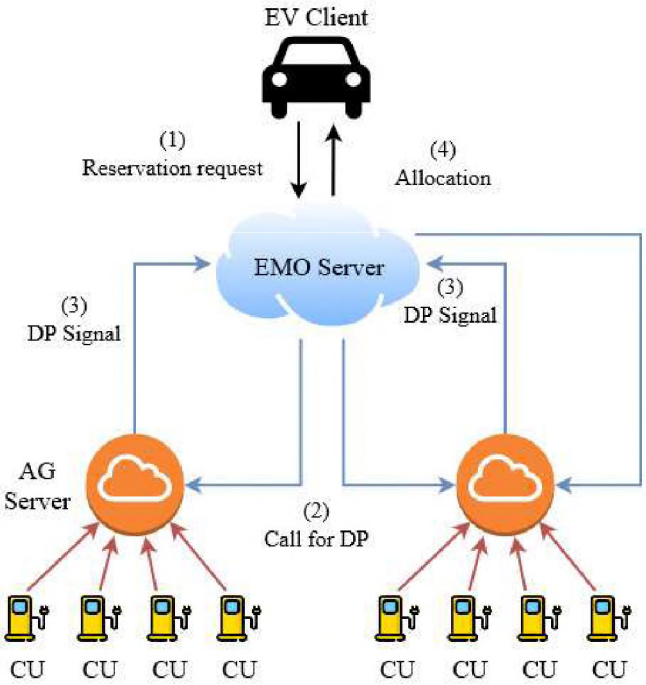

Fig. 3. System architecture for the execution of SR based on DP: (1) The EV user sends a reservation request to the EMO server. (2) The EMO calls aggregators having available chargers for DP. (3) Aggregators calculate cluster-specific cost coefficients through DP. (4) The EMO reserves a charger for the EV, informs the EV user about the reservation, and sends the reference schedule to the reserved CU (via aggregator server).

not within the scope. Nevertheless, a low-latency communication infrastructure between EMO and aggregator servers must be in place to complete the execution of all necessary functions for SR (from the reservation request until a specific cluster selection) within seconds.

The central unit of the envisioned system is the EMO server, which stores the geographical data of the clusters in the UCH. The aggregator servers (AG servers) store the data of charger clusters, such as the connection/reservation status and reference schedules of the CUs. When an EV user accesses the EMO server with a reservation request, the EMO server sends a request (DP call) to the aggregators having available chargers in their clusters for the specified connection period. The clusters that are not within the specified distance of the intended destination of the EV driver are excluded in this step. The AG servers execute the individual dynamic pricing algorithm to provide the EMO with DP signals ($\omega_{c,v}$) based on commitments and capacity constraints of their clusters. The EMO server solves the optimization problem for SR. The optimization outputs (i.e., the selected cluster and reference schedules) are shared with the EV requesting a reservation and the selected cluster's AG server.

B. Optimization model for smart routing

Upon a reservation request, the EMO learns the energy capacity E_v and power limits of the battery of the incoming EV. In these formulations, v index represents a particular EV. In some applications, EV drivers can make reservation requests in advance, such as several hours before visiting the UCH. In this case, arrival SOCs are subject to uncertainties. However, this work investigates the scenarios where the reservation time, R_v, is only a few minutes before arrival A_v. In this case, the information on arrival SOC, $S_v(A_v)$, is assumed to be precise.

The reservation request includes user specifications on the charging demand, such as the target SOC $S_v(D_v)$ for the estimated departure time D_v, lower and upper boundaries of desired SOC range, $\underline{S_v}$ and $\overline{S_v}$. In addition, the drivers specify the energy that they make available for V2G discharge, namely V2G allowance, by selecting parameter $\overline{E_v^-}$. In this case, the aggregators would be allowed to discharge the battery up to $\overline{E_v^-}$ as long as $\underline{S_v}$ specification is respected.

Mathematically, two variables represent the decisions taken through SR. With c representing a particular cluster in the UCH, the first variable $x_{v,c}$ is a binary having the value of 1 for the c that the EV is allocated to and 0 for all other c. The second variable, $p_v(t)$, is the net power that is planned to be supplied along a particular time step $[t, t+\Delta t) \in [A_v, D_v)$ with t and Δt, respectively the time step identifier and length of one time step.

$$min \sum_{t=A_v}^{D_v} \sum_{c=1}^{C} \omega_{c,v}(t) \cdot p_{v,c}(t) \tag{5}$$

$$p_v(t) = \sum_{c}^{C} p_{v,c}(t) \tag{6}$$

$$-P_v^- \cdot x_{v,c} \leq p_{v,c}(t) \leq P_v^+ \cdot x_{v,c} \tag{7}$$

$$\sum_{c=1}^{C} x_{v,c} = 1 \tag{8}$$

$$p_v(t) = p_v^+(t) - p_v^-(t) \tag{9}$$

$$0 \leq p_v^-(t) \leq P_v^- \cdot (1 - x_v^+(t)) \tag{10}$$

$$0 \leq p_v^+(t) \leq P_v^+ \cdot x_v^+(t) \tag{11}$$

$$s_v(t+\Delta t) = s_v(t) + \frac{p_v(t) \cdot \Delta t}{E_v} \tag{12}$$

$$s_v(A_v) = S_v(A_v) \tag{13}$$

$$s_v(D_v) = S_v(D_v) \tag{14}$$

$$\underline{S_v} \leq s_v(t) \leq \overline{S_v} \tag{15}$$

$$\sum_{t=A_v}^{D_v} p_v^-(t) \cdot \Delta t \leq \overline{E_v^-} \tag{16}$$

The objective function (5) represents charging/discharging of EV in all candidate clusters with dedicated variables $p_{v,c}(t)$; in this way, it weighs the candidate charging schedules with corresponding DP signals $\omega_{c,v}(t)$. Since an EV can reside in only one cluster at once, the power to be supplied to the EV at t, $p_v(t)$, has to be equal to one and only one of the $p_{v,c}(t)$ as shown in (6). The constraints (7) and (8) indicate that charging in particular clusters are exclusive cases. For $p_{v,c}(t)$ to have a non-zero value, the binary $x_{v,c}$ representing the corresponding c has to be 1; and only one $x_{v,c}$ can be

1. An EV battery can either be charging or discharging at any given time. Hence, the constraint (9) defines $p_v(t)$ as combination of positive (charging) and negative (discharging) powers, respectively $p_v^+(t)$ and $p_v^-(t)$; and the constraints (10) and (11) expresses their exclusiveness via the binary variable $x_{v,c}^+(t)$, having the value of 1 when charging and 0 when discharging.

The SOC of the EV battery increases when charging and decreases when discharging as defined by (12). The equality functions (13) and (14) enforce the initial SOC and target SOC as optimization constraints. The inequality (15) defines the lower and upper boundaries of the SOC within the optimization instance by considering the parameters provided by the EV driver. Furthermore, the inequality constraint (16) limits the total cumulative V2G discharge according to the V2G allowance $\overline{E_v^-}$.

IV. Real-time charging control

The EMO allocates the incoming EVs into clusters and assigns them reference schedules. Under normal conditions, the aggregators charge the EVs according to their reference schedules. However, DASs and PPLs of the aggregators may prevent following these references. Under conditions that require deviation from the reference schedules, the aggregators update the real-time set points of the CUs in their clusters by considering the connected EVs' flexibility.

A mixed integer quadratic problem (MIQP) formalizes the real-time control (RTC) strategy of the aggregators. Let k be the time when an aggregator, controlling a cluster with N CUs, executes RTC. The specific optimization problem to be solved at k takes into account the events that will (or are expected to) take place within a future period of Δk. By solving this problem, the aggregator calculates the optimal decision (i.e., real-time set points of all CUs in the cluster) that it will implement between $[k, k+\Delta k)$, which we will call the RTC period. The aggregator solves another instance of the optimization problem at $k+\Delta k$ with the new parameters representing the system's updated state. These calculations are repeated periodically.

The SOCs of the EV batteries, $S_u(k)$, are the optimization inputs defining the initial system state. Here u represents a particular CU in the cluster and the connected EV at k. It is worth noting that the initial system state at k is the consequence of the charging/discharging activities before k. Each u has an individual reference value, $S_u^*(k+\Delta k)$, that indicates the desired SOC for the end of the RTC period, $k+\Delta k$. The discharge and charge efficiencies (represented by η_u^- and η_u^+ respectively), the discharge and charge power ratings (represented by P_u^- and P_u^+ respectively), and the energy capacities of the connected EV batteries (represented by E_u) are the input parameters imposing the physical constraints to the RTC problem. In practice, η_u^- and η_u^+ change slightly with discharge/charge power variations. However, for EV chargers with near-ideal efficiencies (e.g., $\eta_u^- = \eta_u^+ \approx 0.95$), the deviations around this standard value are limited and therefore can be neglected in the normal operation range. Likewise, P_u^- and P_u^+ are dependent upon the SOC of the connected battery. The SOC dependency can be significant in ultra-fast charging applications. However, the introduced strategy mainly addresses scenarios with power ratings smaller than $50kW$ where scheduling is relevant. In this case, the SOC change over a single RTC period (e.g., typically few minutes) is rather small, and the variations in P_u^- and P_u^+ are negligible. In the considered scenarios, the charger clusters have power limitations due to DASs or PPLs. These limitations are expressed by the help of two parameters, $\underline{P_c}$ and $\overline{P_c}$, representing the lower and upper bounds of the power limitation of the cluster c. However, it is allowed to violate $\underline{P_c}$ and $\overline{P_c}$ to avoid infeasibility errors. Therefore, these parameters will be mentioned as soft constraints in the following.

The main control variables of RTC problem are the real time charging rates of the charging units in the cluster. In the following, p_u represents the power to be supplied to the EV battery connected to u through the RTC period (i.e, $[k, k+\Delta k)$). s_u is a state variable representing the SOC to be achieved by $k+\Delta k$ as result of p_u. The non-negative slack variable, ϵ, represents the amount of violation of the soft constraints defined by $\underline{P_c}$ and $\overline{P_c}$.

$$\min \underbrace{\sum_{u=1}^{N} \rho_y \cdot (S_u^*(k+\Delta k) - s_u)^2}_{J_y} + \underbrace{\rho_\epsilon \cdot \epsilon}_{J_\epsilon} \tag{17}$$

$$s_u = S_u(k) + \frac{p_u \cdot \Delta k}{E_u} \tag{18}$$

$$p_u = p_u^+ - p_u^- \tag{19}$$

$$0.0 \le p_u^+ \le P_u^+ \cdot x_u^+ \tag{20}$$

$$0.0 \le p_u^- \le P_u^- \cdot (1 - x_u^+) \tag{21}$$

$$\underline{P_c} - \epsilon \le \sum_{u}^{N} \frac{p_u^+}{\eta_u^+} - p_u^- \cdot \eta_u^- \le \overline{P_c} + \epsilon \tag{22}$$

The objective function (17) penalizes two terms. First term, J_y, represents the cost of deviation from the individual reference schedules (i.e., the difference between the achieved SOC and reference SOCs at the end of the RTC period $k+\Delta k$). J_ϵ represents the cost of violation of the soft constraints, determined by $\underline{P_c}$ and $\overline{P_c}$. In these formulations, ρ_y and ρ_ϵ are penalty weights for, respectively, the deviations from the reference schedules and the violation of soft constraints. For such an MIQP to be convex, its Hessian matrix needs to be positive semi-definite. This condition is met when ρ_y has a positive value. There exist several optimization solvers (e.g., CPLEX [26]) guaranteeing global optimality of the convex MIQPs. Nevertheless, the quadratic objective function could also be linearized by a simple technique to reduce computation times and make the problem suitable for a wider variety of solvers. For this purpose, non-negative variables, σ_u, are introduced for each u. In fact, σ_u is equal to the absolute value of the deviation from the reference SOC (i.e., $\sigma_u = |S_u^*(k+\Delta k) - s_u|$). This equality can be expressed via a linear constraint $-\sigma_u \le S_u^*(k+\Delta k) - s_u \le \sigma_u$. Since σ_u is already non-negative, it represents both negative and positive deviations from the reference SOCs, $s_u < S_u^*(k+\Delta k)$ and

$s_u > S_u^*(k+\Delta k)$. Therefore, the same cost factor can be penalized via merely σ_u without quadratic terms.

The constraint (18) describes the relationship between the supplied power and the SOC increase/decrease. Due to the losses in charging/discharging process, the power p_u transferred to/from an EV battery is not equal to the power that the CU withdraws or injects from/to the power system. To transfer p_u to the EV battery, the CU must withdraw $\frac{p_u}{\eta_u^+}$. Conversely, when discharging p_u from the EV battery, the CU injects only $p_u \cdot \eta_u^+$ to the system. Therefore, positive (charging) and negative (discharging) values of p_u are distinguished and represented as p_u^+ and p_u^- respectively. Since a battery can be either charged or discharged at once, it is not allowed for p_u^+ and p_u^- to have a non-zero value simultaneously. To achieve this, binary variables x_u^+ specifying the charging mode of u are added in the optimization model. The constraints (19)-(21) indicate the exclusiveness of charging/discharging for a specific RTC period.

The inequality (22) indicates that the aggregate net power of the cluster must be within a certain operating range. $\underline{P_c}$ and $\overline{P_c}$ define the soft limits of this range. The value of the slack variable, ϵ, is the measure of violation of these soft limits. The non-zero values of ϵ are penalized in the objective function of the RTC model (17). When $\underline{P_c}$ and $\overline{P_c}$ must be enforced as hard constraints, ϵ is constrained to be zero. In this case, the selection of ρ_y and ρ_ϵ is ineffective. When violation of $[\underline{P_c}, \overline{P_c}]$ range is allowed, the ratio $\frac{\rho_\epsilon}{\rho_y}$ can affect the system behavior significantly. The aggregators can update these parameters during the operation if needed. For example, an aggregator that has to pay large penalties in case of deviation from DAS would tend to assign larger values for ρ_ϵ. The aggregator could decrease the value of ρ_ϵ if it estimates that the deviations from individual optimal schedules of the EVs will have more significant cost implications than deviating from DASs. The quantification of the trade-off between these factors is dependent upon the aggregators' business model and thus, is not within the scope of this work. Therefore, both parameters were considered to be 1 in the simulated scenarios.

V. Performance Metrics

This work considers use cases where aggregators in a UCH have DASs and PPLs. The aggregators may have liabilities such as penalty payments to the DSO or energy providers in case of deviation from DASs and PPL violations. However, the penalty that an aggregator would have to pay in such cases is a question of the business model between the aggregator and the relevant external entities. Therefore, the performance in these aspects is not quantified but qualitatively assessed by comparing results obtained under different management concepts.

The quantitative evaluations are conducted by using performance metrics related to the EV users' experience. In the operation of an UCH, DASs or PPLs can affect the rate at which the charging demands are fulfilled and lead to excessive V2G discharge from EV batteries. For the sake of generality of the performance indicators, this work quantifies user experience on the basis of the comparison between what is provided to the EV users (achieved as the consequence of the operation) versus what is promised to them (defined by the reservation agreement). Therefore, it uses unfulfilled demand and unscheduled V2G discharge as performance metrics. Let δ_v and λ_v be the simulation outputs measuring the net energy supplied to the EV battery and cumulative discharge from the EV battery. The unfulfilled demand and unscheduled V2G discharge metrics are calculated as follows.

$$\delta_v^* = (S_v(D_v) - S_v(A_v)) \cdot E_v \tag{23}$$

$$\xi^{UFD} = \sum_{v \in V} max\{0, \delta_v^* - \delta_v\} \tag{24}$$

Above δ_v^* represents the charging demand specified by the driver of v. δ_v^* is a simulation parameter given by the difference between the targeted and arrival SOCs, respectively $S_v(D_v)$ and $S_v(A_v)$. The charging demand is deemed unfulfilled only if the supplied energy (δ_v) is smaller than the amount requested by the driver (δ_v^*). Therefore, the equation (24), which calculates the unfulfilled demand metric, ξ^{UFD}, takes into account only the EVs that received less energy than the amount specified by the driver (i.e., v with $\delta_v^* > \delta_v$).

$$\lambda_v^* = \sum_{t=A_v}^{D_v} \begin{cases} p_v(t) \cdot \Delta t & p_v(t) < 0 \\ 0 & p_v(t) \geq 0 \end{cases} \tag{25}$$

$$\xi^{V2G} = \sum_{v \in V} max\{0, \lambda_v - \lambda_v^*\} \tag{26}$$

The scheduled amount of V2G discharge, λ_v^*, is given by (25). This value is obtained by solving optimization problem (5-16) for smart routing of v and fixed by the reservation agreement. Here, $p_v(t)$ with a negative value indicates that the battery of v is scheduled for discharging in t. V2G discharge is deemed unscheduled only when the discharged amount (λ_v) exceeds the amount specified by the schedule (λ_v^*). As shown in (26), the overall unscheduled V2G, ξ^{V2G}, is the summation of unscheduled V2G of individual EVs.

In a reservation-based service as assumed here, it would be reasonable to pay compensation fees for unfulfilled demand and unscheduled V2G discharge. However, mapping these quantities into currency units is a business question with threefold complexity. First, the compensation fees must be associated with the billing strategy; for example, the payments for fulfilled and unfulfilled parts of the charging demand must be defined. Second, the trade-off between deviations from DASs (or PPL violations) and EV user experience must be quantified. Third, the share of the EMO and the aggregators in the resulting compensation fees must be quantified since both parties affect ξ^{UFD} and ξ^{V2G} by their actions. Since such business questions are not within the scope, this work does not map ξ^{UFD} and ξ^{V2G} into compensation fees and does not distribute them into relevant entities; instead, it takes them as global performance indicators.

VI. Simulation Results

A. Benchmark strategies

In the following, the proposed strategy is applied in test scenarios where aggregators in a UCH have given DASs and

PPLs. To demonstrate the proposed strategy's effectiveness, its performance was compared against relevant benchmark strategies in terms of the metrics introduced in Section V. To best of the authors' knowledge, this is the first work that studies a scenario with a UCH having multiple aggregators and the literature does not provide a model of interaction between the parties involved in such a scenario. Therefore, three assumptions were made about the involved parties. First, an EMO would exist and would be the first point of contact for the incoming EVs, which look for a charging spot in the UCH. Second, each aggregator would apply dynamic pricing for EV charging in its cluster. Third, the charging profile of each EV would be individually scheduled based on the available DP signal(s). By considering the potential functions of the assumed parties, multiple benchmark strategies were selected.

1) Benchmarks without SR function of the EMO: In the proposed strategy, the EMO has smart routing (SR) function; thus, it is responsible for the allocation of incoming EVs into clusters. The charging schedule is jointly optimized with the cluster selection in the proposed SR strategy. In benchmarks without SR, the EMO only informs the EV user about the available clusters, and the EV driver chooses the cluster randomly. The charging schedule of the EV is optimized based on the selected cluster's DP signal.

2) Benchmarks without RTC function of the aggregators: In the proposed RTC strategy, the aggregators recognize the conditions requiring deviations from the individual charging schedules of the EV (i.e., DASs and PPLs) and optimize the real-time charging rates of the CUs in their clusters. In benchmarks without RTC, the aggregators apply the given charging schedules of the EVs without any modifications.

B. Implementation

Pyomo library [27] and optimization solver CPLEX [26] were used for, respectively, modeling and solving the optimization problems. The test scenarios were simulated in Python with 5-min resolution. This is also equal to optimization time steps for both SR and RTC problems. For statistical analyzes of the simulation outputs, functions of numpy library of Python [28] was used. The tested scenarios are introduced in more detail in the following sub-sections.

C. Test case 1: Tracking DASs of the aggregators

The UCH scenario simulated in this part has three aggregators, each controlling 8 CUs with 11 kW power ratings and 95% efficiency. Each aggregator is responsible for supplying energy to a non-residential building with a non-flexible electrical load. When selecting the non-residential building types, heterogeneity in consumption patterns was sought. Therefore, the following building types were considered: a metal company for the first aggregator (AG1), a food production facility for the second (AG2), and a sports hall for the third aggregator (AG3). The load profiles of the non-residential buildings were generated by using the Python package for data handling and scenario generation of city districts and urban energy systems, pycity [29]. The generated load profiles were then scaled such that the peak power demands of the non-residential buildings controlled by AG1, AG2, and AG3, are respectively 56, 76, and 72 kW.

In the tested scenario, 25 EVs use the charging infrastructure of the UCH in 24 hours. The flat price of 0.1 Eur/kWh is assumed for the entire simulation period (i.e., $\kappa_c(t) = 0$ for all t). The EV charging sessions last between 2 and 9 hours. The DASs of aggregators were generated by aiming at load flattening during the periods with EV presence. The non-residential fixed loads and DASs of the aggregators are plotted in Figure 4.

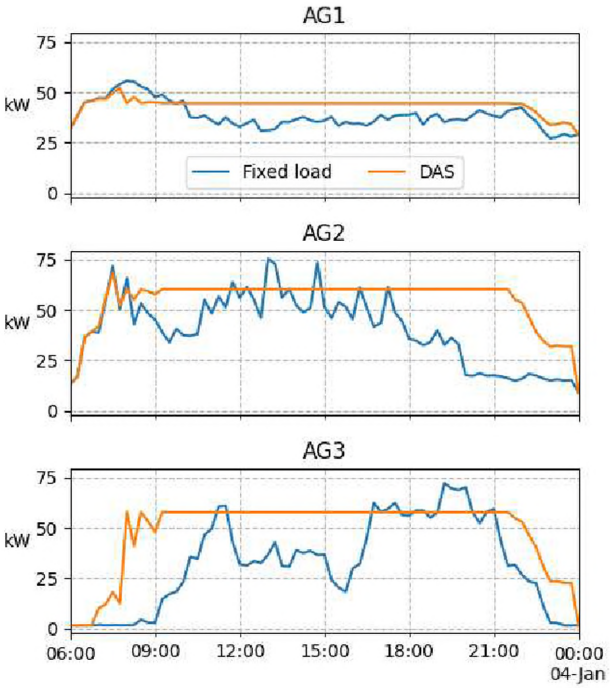

Fig. 4. Non-residential fixed loads and day ahead schedules of the aggregators controlling the charger clusters in the UCH

This scenario was simulated without/with applying smart routing and without/with applying real-time charging control. The resulting net consumption profiles of the aggregators were compared against the DASs given by the scenario in all tests. Figure 5 shows these comparisons. In all subplots, blue and orange colors represent, respectively, operations without and with SR. The subplots on the left show the results of the operation without RTC while the ones on the right are the results of the operation with RTC.

The comparison between left and right subplots shows that RTC improves the DAS tracking performance significantly. As seen in the blue curve of the upper-left subplot, the net consumption of AG1 is mostly more than the amount specified by the DAS. Without RTC, AG1's excessive consumption reaches 25 kW multiple times. The deviations from DAS reduce to near zero values (with a maximum of 11 kW) when AG1 implements RTC. Likewise, the maximum excessive consumption (actual consumption minus DASs) reduces from 37 kW to 15 kW for AG2 and from 26 kW to 14 kW for AG3 when aggregators apply RTC in the scenario without SR.

This article has been accepted for publication in IEEE Transactions on Transportation Electrification. This is the author's version which has not been fully edited and content may change prior to final publication. Citation information: DOI 10.1109/TTE.2022.3208627

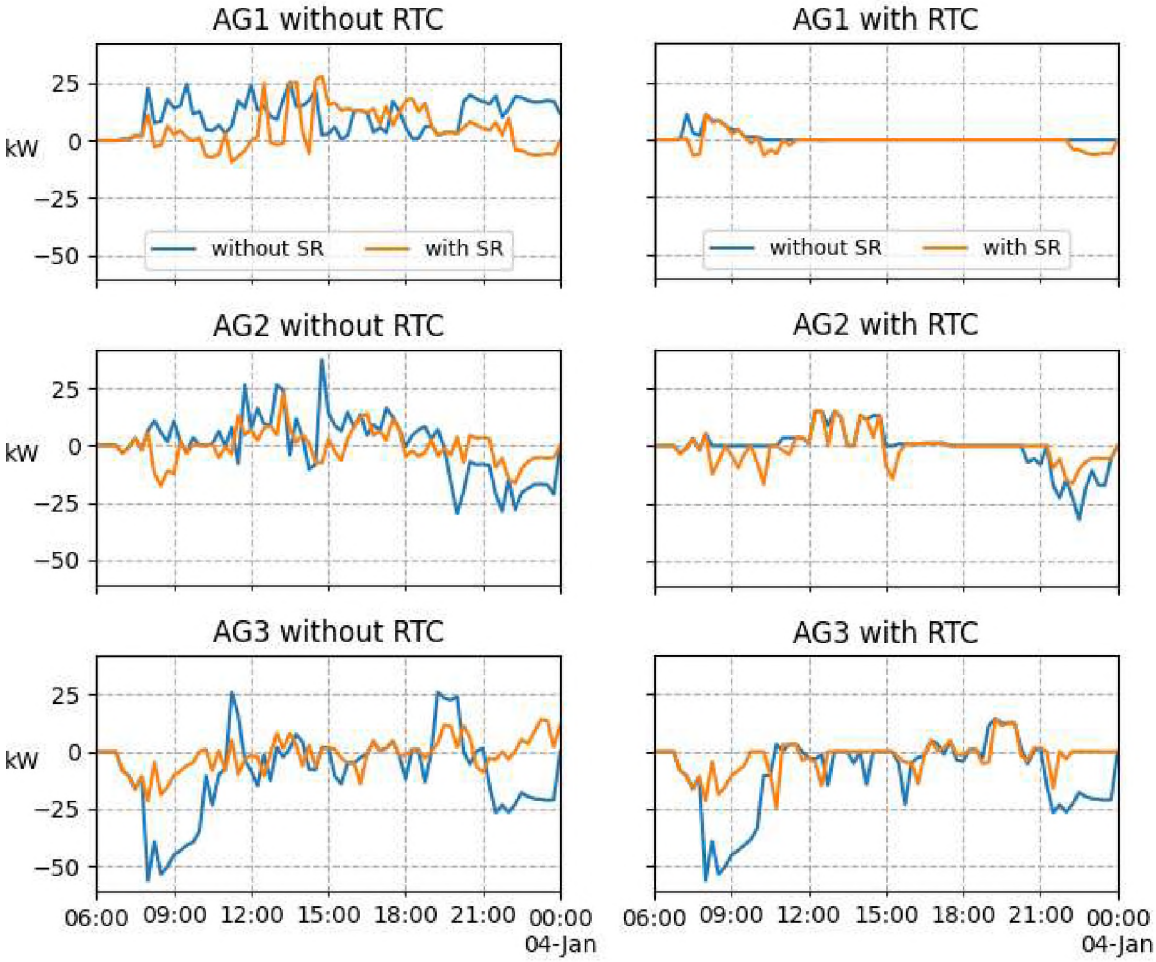

Fig. 5. Deviations from the DASs without RTC versus with SC. Left (without SC) and right (with SC).

Although the RTC helps aggregators track DASs, it is not alone sufficient for the optimization of the system behavior. The constraint (22) often leads to deviations from the charging schedules of the EVs. Therefore, in some cases, the DASs require compromises on the demand fulfillment rates. When aggregators apply RTC in scenarios without SR, the total unfulfilled demand of EVs (ξ^{UFD}) is measured to be 231 kWh. However, this value reduces to 129 kWh thanks to SR. A closer look to the subplots on the left reveals the underlying reason. In all left subplots, the blue curves show deeper and more frequent fluctuations when compared to the orange curves, which means that the deviations from DASs are deeper and more frequent in operation without SR. In other words, the SR leads to a system behavior that resembles the DASs even without RTC. In this case, the aggregators do not have to deviate from individual schedules of the EVs while tracking the DASs. Consequently, the demand fulfillment rates increase when the RTC is combined with SR.

To understand the process that led to higher deviations under operation without SR, the events in the first three hours (7-10AM period) were analyzed carefully. Table I shows the arrival/departure times and the arrival SOCs of the EVs arriving in this period and the clusters that these EVs use. The cluster selections in two cases (i.e., with and without SR) start to differ by 8AM. As seen in Fig. 4, for tracking the DAS in this period, the net power consumption of AG2 must decrease, and the consumption of AG3 must increase. Table I shows that SR allocates all three EVs arriving at 8 AM to the cluster of AG3. In case without SR, the drivers of these EVs randomly select the clusters of AG1 or AG2. Consequently, under the benchmark management without SR, as seen in the subplots on the left of Fig. 5, AG3's cumulative energy consumption in this period is much less than the DAS. With SR, the deviations reduce to near-zero values.

This analysis found evidence for the impact of cluster selections on the demand fulfillment rate. From this, it can also be inferred that the demand fulfillment rates would be variable if the cluster selections of the EVs are not supervised (i.e., random). To analyze the impact of this randomness, the simulations without SR were repeated 100 times, each creating a unique test scenario in terms of the EVs' cluster selections in the UCH. The histograms in Fig. 6 show the distribution of ξ^{UFD} and ξ^{V2G} in these 100 tests. In all tests, the observed ξ^{UFD} is larger than what is observed in the simulation with

TABLE I
EV CONNECTIONS TO THE CLUSTERS CONTROLLED BY THREE AGGREGATORS.

EV	Arrival	Leave	Arrival SOC	Without SR	With SR
1	07:00	15:45	78%	AG1	AG1
2	08:00	10:45	38%	AG2	AG3
3	08:00	15:00	30%	AG1	AG3
4	08:00	13:30	33%	AG2	AG3
5	08:30	12:45	76%	AG2	AG2
6	09:15	14:45	55%	AG3	AG2
7	09:30	16:00	67%	AG1	AG3
8	09:45	16:15	37%	AG3	AG3

SR. Out of 100 tests, only one produces a smaller ξ^{V2G} as compared to the simulation with SR. The mean values of ξ^{UFD} and ξ^{V2G} were measured to be 261 kWh and 41 kWh in 100 tests without SR. These values indicate that SR reduces ξ^{UFD} by 51% on average and ξ^{V2G} by 70%. In light of these findings, it is clear that the performance improvement due to SR is not coincidental because SR consistently outperforms random cluster selections.

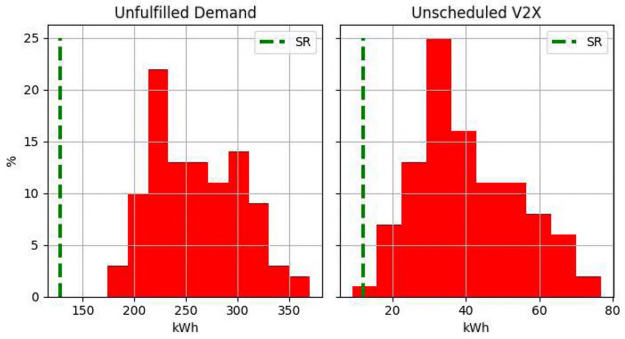

Fig. 6. Histograms of unfulfilled demand and unscheduled V2G transfer without SR.

To summarize, the results of the analyzes indicate the clear benefit of the proposed management concept – which jointly optimizes the allocation and schedules of EVs through SR and controls the real-time operation through RTC – in terms of tracking the DASs of the aggregators. The increased accuracy in DAS tracking is important for grid management as it increases the predictability of the consumer behavior. Furthermore, the applied concept proves to increase the net energy supply to the EVs using the UCH and decrease unscheduled V2G under the controlled operation of aggregators. The improvements in these performance indicators imply significant benefits to the involved parties, such as increased revenues for aggregators and improved experience for EV users.

D. Test case 2: Peak power limits of the aggregators

This test considers an example UCH with 60 identical bidirectional 3-phase AC chargers having an 11 kW power rating and 95% power conversion efficiency (for both charging and discharging). In the main simulation variant, 60 CUs are equally distributed into three clusters, each controlled by one of the aggregators -named AG1, AG2, and AG3. Each aggregator has a PPL of 132 kW, which is equal to 60% of the total installed power of its cluster. In this scenario, V2G discharge essentially indicates a vehicle-to-vehicle energy transfer with the purpose of local balancing under the given PPLs. All aggregators have the same regular time-of-use tariff (κ_c). This tariff is the day ahead market price listed in Germany on January 8th, 2022 [30].

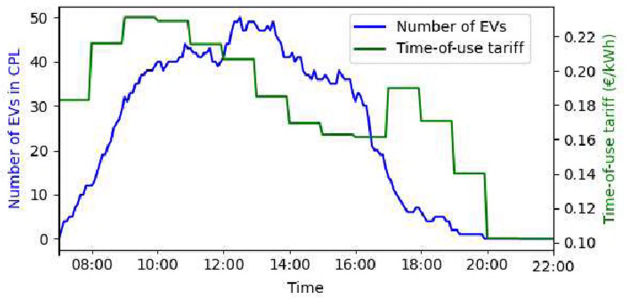

Fig. 7. Number of EVs present in clustered PL and electricity purchase tariff of aggregators.

The considered time-of-use tariff is plotted in Fig. 7 alongside the number of EVs present in the UCH over the simulated period. During this period, 100 EVs visit (each EV once) the UCH between 07:00-22:00. 25% of these EVs stay connected for 1-2 hours, 25% for 2-4 hours, and 50% for 4-6 hours. Their battery capacities are 55 kWh, and their initial SOCs range between 20%-80%. They aim to achieve maximum SOC that could be achieved with 11 kW in the given parking duration, and they permit 5.5 kWh discharging (equal to 10% of the battery capacity of EVs) for V2G purposes.

The introduced scenario was simulated for four cases: without/with SR and without/with RTC. The resulting consumption profiles of the aggregators were plotted in Figure 8. As can be seen in the subplots on the left, the PPLs of the aggregators are often violated unless RTC is implemented to control the operation of the charging units. Such violations occur more often under random cluster selections (i.e., without SR). For AG1, the limits are violated for 145 minutes without SR and only for 25 minutes with SR. AG2's consumption is larger than the given PPL for 145 minutes without SR; it is always within the specified limit under SR.

The comparison between the blue curves on the left and right subplots of Fig. 8 shows that RTC changes the consumption profiles of the aggregators significantly under uncontrolled cluster selection (without SR). On the other hand, the orange curves (i.e., operation with SR) are nearly identical without and with RTC. The underlying reason is that, by jointly optimizing the cluster allocations and reference schedules of the incoming EVs, SR produces reference schedules that are easier to follow. Therefore, the RTC that enforces the peak power constraints requires fewer deviations from the reference schedules under SR. In this case, only 5 kWh of the charging demand remains unfulfilled; it is 113 kWh without SR. In other words, the return of implementing SR is equal to fulfilling the charging demands of four more average customers (each wishing to increase the SOC of their 55 kWh batteries by 50%).

This article has been accepted for publication in IEEE Transactions on Transportation Electrification. This is the author's version which has not been fully edited and content may change prior to final publication. Citation information: DOI 10.1109/TTE.2022.3208627

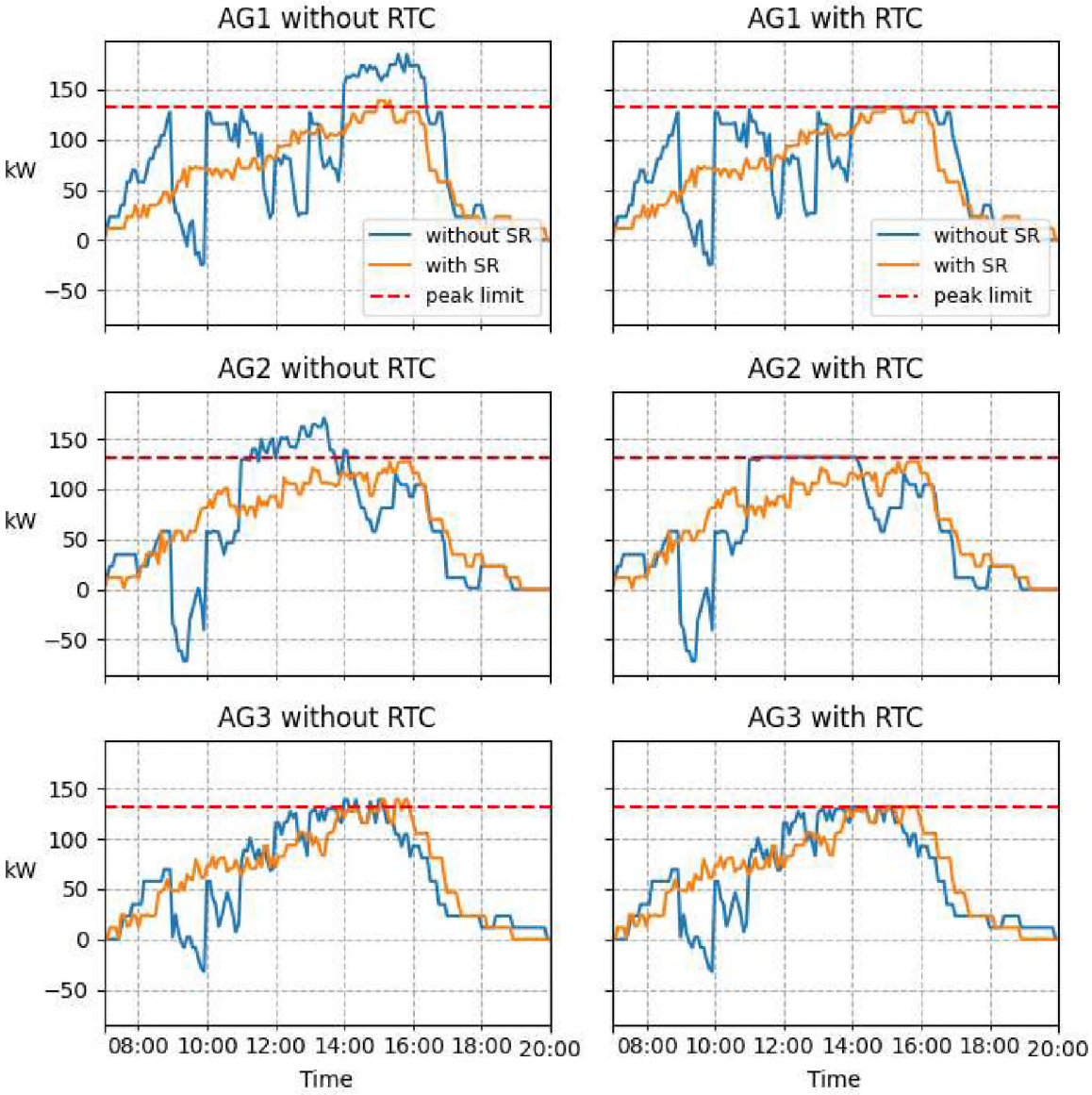

Fig. 8. Cluster profiles versus capacity constraints in 3x20x11kW variant

To investigate the impact of the size of the clusters on the performance metrics, the number of aggregators was modified in different simulation variants. All variants were simulated by applying RTC without and with SR. Tables II and III summarize the comparison between the cases without and with SR in the simulated variants. The observations on demand fulfillment performance are similar in all variants; ξ^{UFD} decreases noticeably thanks to SR. Furthermore, the results indicate that SR not only increases the EV charging potential (i.e., decreasing unfulfilled demand) under capacity constraints but also reduces vehicle-to-vehicle transfer for local balancing purposes. For example, in variant 6x15x11kW, SR reduces the total V2G by 71 kWh. More importantly, it eliminates the unscheduled V2G, ξ^{V2G}, entirely.

TABLE II
UNFULFILLED CHARGING DEMAND FOR ALL SCENARIO VARIANTS WITHOUT AND WITH SR

	Total energy supply		Unfulfilled demand	
Variant	**Without**	**With**	**Without**	**With**
3x20x11kW	2309	2416	113	5
4x15x11kW	2330	2414	92	7
5x12x11kW	2328	2414	94	7
6x10x11kW	2314	2410	108	11

The results denote a limited scenario dependency in the unfulfilled demand and unscheduled V2G. For instance, without SR, ξ^{UFD} is 113 kWh in the scenario variant 3x20x11kW and 92 kWh in the variant 4x15x11kW. However, the difference between ξ^{UFD} measured in two variants reduces to 2 kWh under SR. Likewise, ξ^{V2G} ranges between 8-44 kWh in different variants without SR; it is zero in all variants under SR. From

TABLE III
V2G TRANSFER FOR DIFFERENT SIMULATION VARIANTS

Variant	V2G	Without	With
3x20x11kW	**Scheduled**	272	270
	Unscheduled	15	0
	Total	287	270
4x15x11kW	**Scheduled**	258	239
	Unscheduled	44	0
	Total	302	239
5x12x11kW	**Scheduled**	274	235
	Unscheduled	7	0
	Total	281	235
6x15x11kW	**Scheduled**	273	210
	Unscheduled	8	0
	Total	281	210

these findings, it follows that the proposed strategy responds to the scenario variations consistently while the random cluster selection's performance can show great variability.

The increase in the demand fulfillment under PPLs can have important implications for the system design. This is particularly meaningful when the existing power distribution system lacks sufficient capacity to host a large amount of EV charging demand. In such scenarios, the ability to fulfill charging demands under pronounced PPL reduces the need for grid reinforcement and consequently affects electricity prices.

VII. Computational analysis

For the presented framework to be practicable in real-time applications, the computation times required to solve SR and RTC problems must be sufficiently low. However, there exist no standards that determine the acceptable limits of the computation times in the investigated scenario. Furthermore, the computation time depends upon the available hardware and software. Nevertheless, in the following, it is demonstrated that even moderate computational power (i.e., that of a personal computer, having an Intel(R) Core(TM) i5-8250U CPU @1.80GH and using a CPLEX solver) is sufficient to complete the required computations within reasonably short times.

The time required for solving the SR problem depends upon two factors: the number of time steps in the scheduling problem and the number of candidate clusters in the UCH. The number of time steps is a degree of freedom as the EMO can choose an optimization time step (i.e., Δt in SR model) corresponding to the problem complexity. On the other hand, the EMO has to consider all options within proximity of the intended destination of the driver; thus, it is not allowed to choose the number of candidate clusters in the SR problem. To investigate the impact of this factor, randomly generated SR problems with a fixed number of optimization time steps – 96 steps which correspond to 24 hours with the 15-minute resolution – and a varying number of clusters were solved, and their computation times were observed. 100 trials were made for each case (i.e., a specific number of clusters) to obtain an average measure of the computation time. The mean computation times are depicted in Figure 9a. The results show that it takes about 2 seconds to solve a big optimization problem with 64 candidate clusters, having 13197 constraints and 25382 variables. It is important to note that such a high number of candidate clusters is often unrealistic in small distances to the intended destination of the EV driver. From this, it follows that the computation time of the SR problem in most scenarios is sufficiently short for real-time applications.

As opposed to the SR, RTC is formulated as a single period problem. Thus, the size of the problem is only related to the number of connected EVs. To observe the impact of different problem sizes, the number of the EVs were gradually increased from 2 to 64, and the computation times (of 100 trials per each size) were observed. The mean values of the observed computation times are depicted in Figure 9b. The problem with a cluster size of 64 has 451 variables, with 64 being binary. Even in this case, the mean computation time is below 0.12 seconds. This demonstrates that even computers with moderate performance can quickly solve large RTC problems and adapt the system behavior according to the changes in the real-time conditions, such as connection/disconnection and updated PPLs.

VIII. Conclusion

This paper addresses urban charging hubs (UCHs) where an EV user can access charging services provided by multiple aggregators, each controlling a cluster of EV charging units. In such a scenario, the rules governing 1) the distribution of the EVs into clusters and 2) the distribution of the charging power over time can affect the service quality. This work contributes to the technical literature by defining a decentralized management concept that distributes the control authority to the aggregators, and the electromobility operator (EMO) of a UCH. In this concept, the aggregators control G2V/V2G operations and apply individualized dynamic pricing for EV charging in their clusters. The EMO is entitled to select a cluster for the incoming EVs to minimize the charging cost of its customer. The intelligent behaviors of aggregators and EMO are formalized by dynamic pricing, smart routing (SR) and real-time charging control (RTC) algorithms.

The management concept is demonstrated in two example scenarios where aggregators aim to 1) follow given day ahead schedules and 2) keep their peak consumption under the given limits. The performance of the proposed management concept is compared against benchmark strategies without SR and RTC. The simulation results show that the proposed management concept tracks the day ahead schedules with remarkably higher accuracy. In scenarios where charger clusters have peak consumption power limitations, the proposed strategy removes the unscheduled discharge from EV batteries and reduces the unfulfilled charging demand by up to 97% as compared to the amounts recorded under benchmark strategies without SR.

In a real-world application, tracking day ahead schedules with higher accuracy makes the behavior of charger clusters more predictable and thus facilitates dealing with the capacity constraints of the power system. Furthermore, the reduction in unfulfilled charging demand and unscheduled V2G discharge is strongly related to EV users' satisfaction with charging services. Therefore, the proposed strategy proposes significant benefits for grid-oriented coordinated charging and EV users' experience.

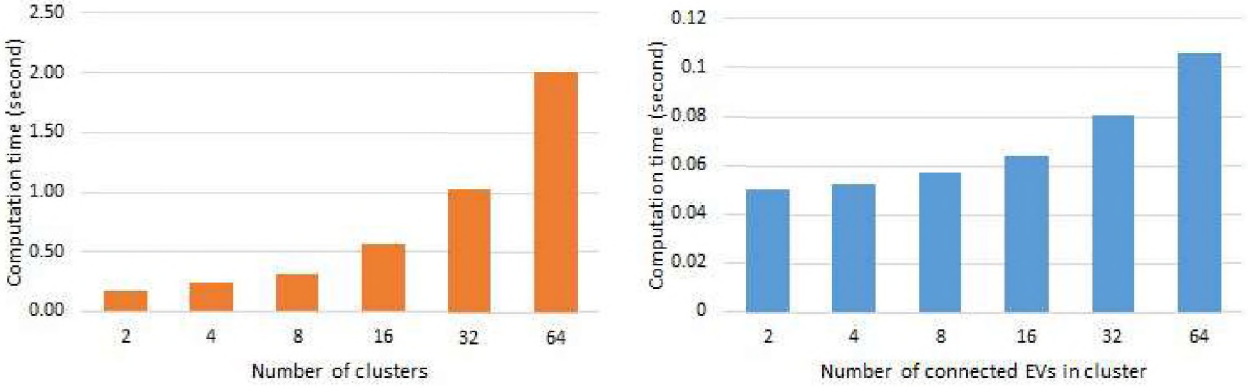

(a) Smart routing

(b) Real time charging control

Fig. 9. Mean computation time for solving optimization problems. (a) Smart routing (b) Real time charging control

REFERENCES

[1] Federal Motor Transport Authority (KBA), "Vehicle Registrations in December 2021 - Annual Balance Sheet," Retrieved from https://www.kba.de/DE/Presse/Pressemitteilungen, 2022, accessed: 2022-07-27.

[2] Norwegian Electric Car Association, "Norwegian EV market," Available at https://elbil.no/english/norwegian-ev-market/ (2022/03/11), 2021.

[3] E. Vega-Fuentes and M. Denai, "Enhanced Electric Vehicle Integration in the UK Low-Voltage Networks With Distributed Phase Shifting Control," *IEEE Access*, vol. 7, pp. 46 796–46 807, 2019.

[4] N. Azizan Ruhi, K. Dvijotham, N. Chen, and A. Wierman, "Opportunities for price manipulation by aggregators in electricity markets," *IEEE Transactions on Smart Grid*, vol. 9, no. 6, pp. 5687–5698, 2018.

[5] A. Zahedmanesh, K. M. Muttaqi, and D. Sutanto, "A cooperative energy management in a virtual energy hub of an electric transportation system powered by pv generation and energy storage," *IEEE Transactions on Transportation Electrification*, vol. 7, no. 3, pp. 1123–1133, 2021.

[6] J. A. P. Lopes, F. J. Soares, and P. M. R. Almeida, "Integration of Electric Vehicles in the Electric Power System," *Proceedings of the IEEE*, vol. 99, no. 1, pp. 168–183, 2011.

[7] M. S. El Nozahy and M. M. A. Salama, "A Comprehensive Study of the Impacts of PHEVs on Residential Distribution Networks," *IEEE Transactions on Sustainable Energy*, vol. 5, no. 1, pp. 332–342, 2014.

[8] Y. Guo, J. Xiong, S. Xu, and W. Su, "Two-Stage Economic Operation of Microgrid-Like Electric Vehicle Parking Deck," *IEEE Transactions on Smart Grid*, vol. 7, no. 3, pp. 1703–1712, 2016.

[9] C. B. Saner, A. Trivedi, and D. Srinivasan, "A Cooperative Hierarchical Multi-Agent System for EV Charging Scheduling in Presence of Multiple Charging Stations," *IEEE Transactions on Smart Grid*, vol. 13, no. 3, pp. 2218–2233, 2022.

[10] K. Kaur, M. Singh, and N. Kumar, *IEEE Systems Journal, title=Multiobjective Optimization for Frequency Support Using Electric Vehicles: An Aggregator-Based Hierarchical Control Mechanism, year=2019, volume=13, number=1, pages=771-782, doi=10.1109/JSYST.2017.2771948.*

[11] Z. Yi, Y. Xu, H. Wang, and L. Sang, "Coordinated Operation Strategy for a Virtual Power Plant With Multiple DER Aggregators," *IEEE Transactions on Sustainable Energy*, vol. 12, no. 4, pp. 2445–2458, 2021.

[12] Z. Li, S. Wang, X. Zheng, F. de León, and T. Hong, "Dynamic Demand Response Using Customer Coupons Considering Multiple Load Aggregators to Simultaneously Achieve Efficiency and Fairness," *IEEE Transactions on Smart Grid*.

[13] K. Kok and A. Subramanian, "Fast locational marginal pricing for congestion management in a distribution network with multiple aggregators," in *CIRED 2019 Conference*. AIM, 2019.

[14] E. Yudovina and G. Michailidis, "Socially optimal charging strategies for electric vehicles," *IEEE Transactions on Automatic Control*, vol. 60, no. 3, pp. 837–842, 2015.

[15] A. Abdulaal, M. H. Cintuglu, S. Asfour, and O. A. Mohammed, "Solving the Multivariant EV Routing Problem Incorporating V2G and G2V Options," *IEEE Transactions on Transportation Electrification*, vol. 3, no. 1, pp. 238–248, March 2017.

[16] M. N. Alam, S. Chakrabarti, and A. Ghosh, "Networked Microgrids: State-of-the-Art and Future Perspectives," *IEEE Transactions on Industrial Informatics*, vol. 15, no. 3, pp. 1238–1250, 2019.

[17] D. Wang, X. Guan, J. Wu, P. Li, P. Zan, and H. Xu, "Integrated Energy Exchange Scheduling for Multimicrogrid System With Electric Vehicles," *IEEE Transactions on Smart Grid*, vol. 7, no. 4, pp. 1762–1774, 2016.

[18] A. Singh, B. K. Sethi, D. Singh, and R. K. Misra, "Shapley Value Method and Stochastic Dantzig–Wolfe Decomposition for Decentralized Scheduling of Multimicrogrid," *IEEE Systems Journal*, vol. 16, no. 2, pp. 2672–2683, 2022.

[19] A. Y. Ali, A. Hussain, J.-W. Baek, and H.-M. Kim, "Optimal operation of networked microgrids for enhancing resilience using mobile electric vehicles," *Energies*, vol. 14, no. 1, 2021. [Online]. Available: https://www.mdpi.com/1996-1073/14/1/142

[20] X. Chen, H. Wang, F. Wu, Y. Wu, M. C. González, and J. Zhang, "Multimicrogrid Load Balancing Through EV Charging Networks," *IEEE Internet of Things Journal*, vol. 9, no. 7, pp. 5019–5026, 2022.

[21] E. Gümrükcü, F. Ponci, A. Monti, G. Guidi, S. D'Arco, and J. A. Suul, "Optimal load management strategy for large electric vehicle charging stations with undersized charger clusters," *IET Electrical Systems in Transportation*, 2021. [Online]. Available: https://ietresearch.onlinelibrary.wiley.com/doi/abs/10.1049/els2.12037

[22] E. Gümrükcü, E. Asadollahi, C. Joglekar, F. Ponci, A. Monti, G. Guidi, S. D'Arco, and J. A. Suul, "Optimal Management for Megawatt Level Electric Vehicle Charging Stations with a Grid Interface Based on Modular Multilevel Converter," *IEEE Access*, pp. 1–1, 2021.

[23] T. M. Aljohani, A. F. Ebrahim, and O. A. Mohammed, "Dynamic Real-Time Pricing Mechanism for Electric Vehicles Charging Considering Optimal Microgrids Energy Management System," *IEEE Transactions on Industry Applications*, vol. 57, no. 5, pp. 5372–5381, 2021.

[24] Ö. Okur, P. Heijnen, and Z. Lukszo, "Aggregator's business models in residential and service sectors: A review of operational and financial aspects."

[25] H. Golmohamadi, "Agricultural demand response aggregators in electricity markets: Structure, challenges and practical solutions- a tutorial for energy experts," *Technology and Economics of Smart Grids and Sustainable Energy*, vol. 5, no. 1, p. 17, 2020.

[26] CPLEX, Retrieved from https://www.ibm.com/de-de/products/ilog-cplex-optimization-studio, accessed: 2020-04-01.

[27] W. E. Hart, C. D. Laird, J.-P. Watson, D. L. Woodruff, G. A. Hackebeil, B. L. Nicholson, and J. D. Siirola, *Pyomo–Optimization Modeling in Python*, 2nd ed. Springer Science & Business Media, 2017, vol. 67.

[28] T. E. Oliphant, *A guide to NumPy*. Trelgol Publishing USA, 2006.

[29] J. Schiefelbein, J. Rudnick, A. Scholl, P. Remmen, M. Fuchs, and D. Müller, "Automated urban energy system modeling and thermal building simulation based on openstreetmap data sets," *Building and environment*, vol. 149, pp. 630–639, 2019.

[30] Nord Pool, "Day-ahead prices in DE-LU region," Retrieved from https://www.nordpoolgroup.com/, accessed: 2022-01-15.